Excitability in optically injected microdisk lasers with phase controlled excitatory and inhibitory response

Koen Alexander,[1,3] Thomas Van Vaerenbergh,[1,3,*] Martin Fiers,[1,3] Pauline Mechet,[1,3] Joni Dambre,[2] and Peter Bienstman[1,3]

[1]*Photonics Research Group (INTEC), Ghent University - imec, Sint-Pietersnieuwstraat 41, B-9000 Ghent, Belgium*
[2]*Electronics and Information Systems (ELIS), Ghent University, Sint-Pietersnieuwstraat 41, B-9000 Ghent, Belgium*
[3]*Center for Nano- and Biophotonics (NB-Photonics), Ghent University, Sint-Pietersnieuwstraat 41, B-9000 Ghent, Belgium*
**Corresponding author: thomas.vanvaerenbergh@intec.ugent.be*

Abstract: We demonstrate class I excitability in optically injected microdisk lasers, and propose a possible optical spiking neuron design. The neuron has a clear threshold and an integrating behavior, leading to an output rate-input rate dependency that is comparable to the characteristic of sigmoidal artificial neurons. We also show that the optical phase of the input pulses has influence on the neuron response, and can be used to create inhibitory, as well as excitatory perturbations.

OCIS codes: (200.4700) Optical neural systems; (130.5990) Semiconductors; (140.3520) Lasers, injection-locked; (230.1150) All-optical devices

References and links

1. W. Maass, T. Natschläger, and H. Markram, "Real-time computing without stable states: a new framework for neural computation based on perturbations," Neural Comput. **14**, 2531–2560 (2002).
2. H. Jaeger, "Harnessing nonlinearity: predicting chaotic systems and saving energy in wireless communication," Science **304**, 78–80 (2004).
3. B. Schrauwen, M. D'Haene, D. Verstraeten, and J. V. Campenhout, "Compact hardware liquid state machines on FPGA for real-time speech recognition," Neural Netw. **21**, 511–23 (2008).
4. S. Ghosh-Dastidar and H. Adeli, "Spiking neural networks," Int. J. Neural Syst. **19**, 295–308 (2009).
5. W. Maass, "Networks of spiking neurons: the third generation of neural network models," Neural Netw. **10**, 1659–1671 (1997).
6. E. M. Izhikevich, *Dynamical Systems in Neuroscience: The Geometry of Excitability and Bursting (Computational Neuroscience)* (The MIT Press, 2006), 1st ed.
7. P. Merolla, J. Arthur, F. Akopyan, N. Imam, R. Manohar, and D. S. Modha, "A digital neurosynaptic core using embedded crossbar memory with 45pj per spike in 45nm," in "Custom Integrated Circuits Conference (CICC), 2011 IEEE," (IEEE, San Jose, 2011), 1–4.
8. M. A. Nahmias, B. J. Shastri, A. N. Tait, S. Member, and P. R. P. Fellow, "A leaky integrate-and-fire laser neuron for ultrafast cognitive computing," IEEE J. Sel. Top. Quantum Electron. **16**, 1–12 (2013).
9. S. Wieczorek, B. Krauskopf, and D. Lenstra, "Multipulse excitability in a semiconductor laser with optical injection," Phys. Rev. Lett. **88**, 063901 (2002).
10. D. Goulding, S. Hegarty, O. Rasskazov, S. Melnik, M. Hartnett, G. Greene, J. McInerney, D. Rachinskii, and G. Huyet, "Excitability in a quantum dot semiconductor laser with optical injection," Phys. Rev. Lett. **98**, 153903 (2007).
11. M. Turconi, B. Garbin, M. Feyereisen, M. Giudici, and S. Barland, "Control of excitable pulses in an injection-locked semiconductor laser," Phys. Rev. E **88**, 022923 (2013).
12. M. A. Nahmias, A. N. Tait, B. J. Shastri, and P. R. Prucnal, "An evanescent hybrid silicon laser neuron," in "Proc. IEEE Photonics Conference (IPC)," (IEEE, Seattle, 2013), 93–94.

#197315 - $15.00 USD Received 6 Sep 2013; revised 9 Oct 2013; accepted 13 Oct 2013; published 24 Oct 2013

13. L. Gelens, S. Beri, and J. Danckaert, "Phase-space approach to directional switching in semiconductor ring lasers," Appl. Phys. 1–9 (2009).
14. S. Beri, L. Mashall, L. Gelens, G. Van der Sande, G. Mezosi, M. Sorel, J. Danckaert, and G. Verschaffelt, "Excitability in optical systems close to Z2-symmetry," Phys. Lett. A **374**, 739–743 (2010).
15. L. Gelens, S. Beri, G. Sande, G. Verschaffelt, and J. Danckaert, "Multistable and excitable behavior in semiconductor ring lasers with broken Z2-symmetry," Eur. Phys. Journ. D **58**, 197–207 (2010).
16. W. Coomans, L. Gelens, S. Beri, J. Danckaert, and G. Van der Sande, "Solitary and coupled semiconductor ring lasers as optical spiking neurons," Phys. Rev. E **84**, 1–8 (2011).
17. Y. De Koninck, K. Huybrechts, G. Van der Sande, J. Danckaert, R. Baets, and G. Morthier, "Nonlinear dynamics of asymmetrically coupled microdisk lasers," in "LEOS Annual Meeting Conference Proceedings, 2009. LEOS'09. IEEE," (IEEE, 2009), 503–504.
18. J. Van Campenhout, P. Romeo, D. Van Thourhout, C. Seassal, P. Regreny, L. Di Cioccio, J.-M. Fedeli, and R. Baets, "Design and optimization of electrically injected InP-based microdisk lasers integrated on and coupled to a SOI waveguide circuit," J. Lightw. Technol. **26**, 52–63 (2008).
19. P. Mechet, S. Verstuyft, T. D. Vries, T. Spuesens, P. Regreny, D. V. Thourhout, G. Roelkens, and G. Morthier, "Unidirectional III-V microdisk lasers heterogeneously integrated on SOI," Opt. Express **21**, 1988–1990 (2013).
20. S. Keyvaninia, M. Muneeb, S. Stanković, P. J. Van Veldhoven, D. Van Thourhout, and G. Roelkens, "Ultra-thin DVS-BCB adhesive bonding of III-V wafers, dies and multiple dies to a patterned silicon-on-insulator substrate," Opt. Mater. Express **3**, 35 (2012).
21. S. Stankovicić, R. Jones, J. Heck, M. Sysak, D. Van Thourhout, and G. Roelkens, "Die-to-die adhesive bonding procedure for evanescently-coupled photonic devices," Electrochem. Solid-State Lett. **14**, H326 (2011).
22. L. Liu, R. Kumar, K. Huybrechts, G. Roelkens, E.-j. Geluk, T. Spuesens, T. D. Vries, P. Regreny, D. V. Thourhout, R. Baets, and G. Morthier, "An ultra-small, low-power, all-optical flip-flop memory on a silicon chip," Nat. Photonics **4**, 1–6 (2010).
23. T. Van Vaerenbergh, M. Fiers, P. Mechet, T. Spuesens, R. Kumar, G. Morthier, B. Schrauwen, J. Dambre, and P. Bienstman, "Cascadable excitability in microrings," Opt. Express **20**, 20292–20308 (2012).
24. M. Fiers, T. Van Vaerenbergh, K. Caluwaerts, D. Vande Ginste, B. Schrauwen, J. Dambre, and P. Bienstman, "Time-domain and frequency-domain modeling of nonlinear optical components at the circuit-level using a node-based approach," J. Opt. Soc. Am. B **29**, 896–900 (2012).
25. M. Sorel, P. Laybourn, A. Scirè, S. Balle, G. Giuliani, R. Miglierina, and S. Donati, "Alternate oscillations in semiconductor ring lasers," Opt. Lett. **27**, 1992–1994 (2002).
26. M. Sorel, G. Giuliani, a. Scire, R. Miglierina, S. Donati, and P. Laybourn, "Operating regimes of gaas-algaas semiconductor ring lasers: experiment and model," IEEE J. Quant. Electron. **39**, 1187–1195 (2003).
27. J. Van Campenhout, "Thin-film microlasers for the integration of electronic and photonic integrated circuits," Ph.D. thesis, UGent (2007-2008).
28. W. Coomans, S. Beri, G. V. D. Sande, L. Gelens, and J. Danckaert, "Optical injection in semiconductor ring lasers," Phys. Rev. A **81**, 033802 (2010).
29. S. Wieczorek, B. Krauskopf, T. Simpson, and D. Lenstra, "The dynamical complexity of optically injected semiconductor lasers," Phys. Rept. **416**, 1–128 (2005).
30. K. Vandoorne, J. Dambre, D. Verstraeten, B. Schrauwen, and P. Bienstman, "Parallel reservoir computing using optical amplifiers," IEEE Trans. Neural Netw. **22**, 1469–1481 (2011).
31. M. R. Watts, J. Sun, C. DeRose, D. C. Trotter, R. W. Young, and G. N. Nielson, "Adiabatic thermo-optic Mach-Zehnder switch," Opt. Lett. **38**, 733–5 (2013).

1. Introduction

Artificial Neural Networks (ANNs) are networks that are somehow inspired by biological neural networks. Using fundamentally different computational principles, ANNs can outperform conventional computer architectures in a variety of tasks, such as autonomous signal generation, control functions in robotics, chaotic time series prediction and speech recognition [1–3]. Spiking Neural Networks (SSNs) have become increasingly popular during the last decade [4, 5]. By transferring information using pulses, they more accurately mimic the behavior of biological neurons than previous generations of neural networks [6].

Functional SNNs have recently been realized in electronics [3, 7]. Notwithstanding the potential of these electronic systems, they are subject to a fundamental bandwidth fan-in product limit. Using photonics, higher speeds and bandwidths are possible in principle. Neural networks operating at time scales that are orders of magnitude faster than their biological and electronic counterparts could be possible [8].

#197315 - $15.00 USD Received 6 Sep 2013; revised 9 Oct 2013; accepted 13 Oct 2013; published 24 Oct 2013

Optical SNNs should consist of excitable components. A suitable excitability mechanism is found in optically injected single-mode semiconductor lasers [9–11], as they are, near the threshold for injection locking, class I excitable, phenomenologically resembling the well-known Leaky Integrate-and-Fire (LIF) model of a spiking neuron [6]. Current research focuses on the usage of similar behaving optical components in an integrated circuit. Recently, Nahmias et al. [8] proposed in simulation a platform based on excitable vertical cavity surface-emitting lasers. However, the interconnection of the different optical neurons needs to be done off-chip. An approach more amenable to integration is proposed in [12], in which an RF connection between a photodetector and a hybrid laser allows for both inhibitory and excitatory inputs. A fully integrated all-optical alternative is demonstrated both numerically and experimentally for Semiconductor Ring Lasers (SRLs) by Gelens, Coomans et al. [13–16]. SRLs support two counterpropagating modes, which are both linearly and non-linearly coupled to each other by intermodal coupling and cross-gain saturation, respectively. For a restricted phase range of the intermodal coupling coefficient, alternate oscillations (AO) will appear. If the laser is operated in the unidirectional regime with two stable states, near the onset of this AO regime, theoretically, excitability is expected, but as a drawback of the symmetry of the system, the attraction basins of both stable states are equal in size and, consequently, there will be a competition between mode-hopping events between both stable states and excitable excursions [13]. This drawback can be solved by inducing an asymmetry in the intermodal coupling [14–16]. This causes the basin of one of these equilibria to shrink drastically, making the state metastable. For very specific phases of the intermodal coupling coefficients, the basin of the remaining state will have a spiralling appearance, allowing for a more reliable type of excitability. However, this mechanism still has a couple of disadvantages. For instance, strong input perturbations can cause a multipulse excitation [16], with the number of pulses increasing with then input perturbation strength, which is both not compatible with the more traditional LIF behaviour [6]. Moreover, the fact that the phase of the linear coupling is of such critical influence, raises questions about the practical feasibility of this method.

Microdisk lasers behave phenomenologically identically to SRLs [16,17]. As a consequence, inducing a reflection asymmetry also reveals the excitability mechanism found in SRLs. However, in this paper, to obtain class I excitability in these microdisk lasers we induce asymmetry in the system equations in a different way, i.e., by optical injection in one of the two counterpropagating modes, giving rise to the same excitability mechanism as found in single-mode semiconductor lasers [9–11]. An advantage of the circular cavity sytem is that we can use the signal of the suppressed mode as output of the system, resulting in a well-behaved input-output behavior. In contrast to asymmetric SRLs, which behave as resonator neurons, the microdisks act as integrating neurons, similar to LIF neurons [6]. Moreover, we show that by using the optical phase, pulse trains can be created that have excitatory or inhibitory effects on the excitability mechanism.

Hence, the microdisk laser forms a promising building block for large photonic SNNs. Indeed, these microdisk lasers are fabricated using hybrid III-V on silicon technology [18, 19], which makes the neurons highly scalable through techniques as wafer bonding [12, 20, 21]. Furthermore, they have a smaller footprint and lower power usage than many other integrated lasers and operate at higher speed [22]. Being active components in a hybrid platform, these lasers have the advantage of being able to compensate for losses, for example in a hybrid neural network with passive excitable components, such as microring resonators [23], paving the way for integrated ultrafast, all-optical neural networks. This type of networks could be useful for a growing number of applications that require lower latencies outside the abilities of the fastest electronic circuits, including processing of the RF spectrum or ultrafast control [12].

The rest of this paper is structured as follows. The model used for the microdisk laser is

#197315 - $15.00 USD Received 6 Sep 2013; revised 9 Oct 2013; accepted 13 Oct 2013; published 24 Oct 2013

first introduced. The effect of optical injection on the laser dynamics is then presented. This optical injection study is interpreted to predict class I excitability. A possible neuron geometry is introduced. Threshold behavior, phase dependency and the response to one or more equidistant pulse trains are then investigated. Simulations were done using Caphe, a nonlinear circuit simulator developed in our group [24].

2. The microdisk laser

The microdisk lasers simulated and discussed in this paper, consist of a disk-shape InP laser cavity, with a InAsP quantum well gain section, bonded on top of a Silicon-On-Insulator (SOI) substrate [18, 19]. The modes are evanescently coupled to a silicon waveguide in the SiO_2-substrate layer. In Fig. 1, a sketch of the microdisk laser is shown in the inset. The single-mode disk supports two counter-propagating *whispering gallery* modes, which are evanescently coupled to a silicon waveguide in the SOI layer. The lasers are electrically pumped and can be subject to optical injection from both sides through the coupling waveguide. One can describe the dynamic behavior of a microdisk laser using a set of coupled rate equations, in the slowly varying amplitude approach, representing the evolution of the complex mode amplitudes, E^+ and E^- ($|E_\pm|^2$ is the number of photons in the mode, while the optical field oscillates with an additional $e^{-j\omega_{in}t}$-dependency), and the number of free carriers, N, in the cavity [17, 19, 25]:

$$\frac{dE^+}{dt} = \frac{1}{2}(1-j\alpha)\left(G^+ - \frac{1}{\tau_p}\right)E^+ + j\Delta\omega E^+ + CE^- - j\frac{\kappa\sqrt{\tau}}{\sqrt{\hbar\omega_0}}E_{in,1} \quad (1)$$

$$\frac{dE^-}{dt} = \frac{1}{2}(1-j\alpha)\left(G^- - \frac{1}{\tau_p}\right)E^- + j\Delta\omega E^- + CE^+ - j\frac{\kappa\sqrt{\tau}}{\sqrt{\hbar\omega_0}}E_{in,2} \quad (2)$$

$$\frac{dN}{dt} = \frac{\eta I}{q} - \frac{N}{\tau_c} - G^+\left|E^+\right|^2 - G^-\left|E^-\right|^2 \quad (3)$$

$$G^\pm = \frac{\Gamma g_N (N-N_0)}{1+\Gamma\varepsilon_{NL}\left(|E^\pm|^2 + 2|E^\mp|^2\right)} \quad (4)$$

In Eqs. (1) and (2), α is the line broadening factor, τ_p the photon lifetime in the cavity, τ is the roundtrip time of the cavity, $\Delta\omega = \omega_{in} - \omega_0$ the detuning between the input light ω_{in} and the free-running cavity frequency ω_0, C is the complex intermodal coupling coefficient. This linear coupling can be due to inhomogeneities in absorption and refractive index along the disk, such as surface roughness, or due to external reflections on grating couplers or fiber facets [19, 22]. κ is the coupling with the waveguide. $E_{in,1,2}$ are the complex amplitudes of the optical inputs ($|E_{in,1,2}|^2$ is the power in the waveguide). Equation (3) describes the evolution of the number of free carriers. I is the injected current, q the elementary charge, η a current efficiency factor, and τ_c the carrier lifetime. $G^\pm$ are the gain coefficients of the modes, g_N is the differential gain, N_0 the transparency threshold of free carriers and Γ the confinement factor. The denominator in Eq. (3) includes cross- and self-gain modulation, ε_{NL} is called the nonlinear gain suppression coefficient. The number of photons that couples from the modes into the output mode per roundtrip time τ can be written as $|\tau\kappa E^\pm|^2$. The output power is thus $\frac{\hbar\omega_0\kappa^2\tau^2}{\tau}|E^\pm|^2$. Taking into account the input amplitudes this yields:

$$E_{out,1} = E_{in,2} - j\kappa\sqrt{\hbar\omega_0\tau}E^- \quad (5)$$

$$E_{out,2} = E_{in,1} - j\kappa\sqrt{\hbar\omega_0\tau}E^+ \quad (6)$$

The bifurcation diagram in Fig. 1 shows the different operating regimes of the laser, as a function of the current I. Regime I is below lasing threshold. In the bidirectional regime (II),

#197315 - $15.00 USD Received 6 Sep 2013; revised 9 Oct 2013; accepted 13 Oct 2013; published 24 Oct 2013

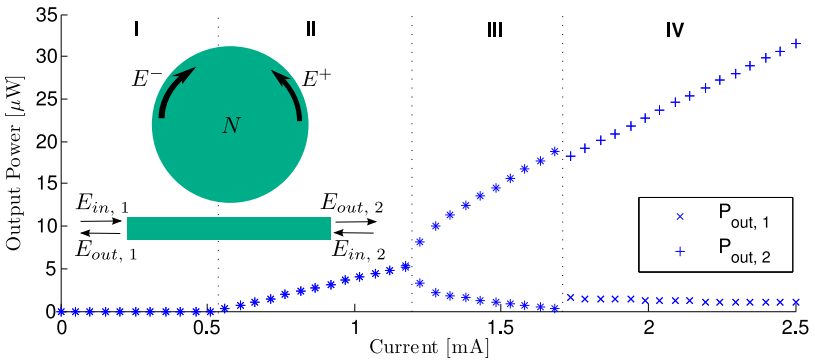

Fig. 1. Bifurcation diagram of the microdisk laser. For both output powers $P_{out,\,i} = |E_{out,\,i}|^2$, the extrema are plotted. If the output is constant, maximum and minimum power are equal and the markers overlap. If the output power oscillates, two markers are plotted per current, per mode. Inset: geometry of the microdisk laser.

the energy in both modes is equal, due to the linear intermodal coupling. At very large currents, the cross-gain modulation overrules the linear intermodal coupling and consequently induces a purely unidirectional regime (IV), where one mode carries more power than the other. If the phase ϕ_C of the intermodal coupling is close to $\frac{\pi}{2}$, in between those two regimes, the combination of cross-gain modulation and intermodal coupling results in a current regime with AO (III) [13,25]. Although a detailed inventarisation of C-values and a corresponding experimental characterization of the oscillatory regime still needs to be done, the frequency of the oscillations is known to be in the GHz range [19] and depends on the magnitude of $|C|$. The rate equation model is developed and thoroughly validated in the case of SRLs [25,26]. In this paper, we use the model parameters for a typical microdisk proposed in [17,27] (table 1), to have qualitative correspondence, on the right order of magnitude, between the numerically obtained diagrams and experimental data obtained in, e.g., [19] or [22].

Table 1. Model parameters used in this paper are based on the values and definitions proposed in [27] and [17]. Comparable values can be found in [19].

Parameter	**Symbol**	**Value**	**Unit**	**Reference**
Resonance wavelength	$\lambda_0 = \frac{2\pi c}{\omega_0}$	1.55	μm	
Line broadening factor	α	3		[27]
Photon lifetime	τ_p	4.17	ps	[27]
Radius microdisk	R	5	μm	[17]
Cavity roundtrip time	τ	350	fs	[17]
Intermodal coupling	C	$0.449 + 2.82j$	GHz	[17]
Amplitude coupling to the waveguide	κ	171.4	GHz	[17]
Current efficiency	η	0.5		[17]
Group velocity of the mode	v_g	$8.82 \cdot 10^7$	$\frac{\mathrm{m}}{\mathrm{s}}$	[17]
Carrier lifetime	τ_c	600	ps	[27]
'Effective' differential gain	Γg_N	982.3	kHz	[27]
'Effective' nonlinear gain suppression	$\Gamma \varepsilon_{NL}$	$1.96 \cdot 10^{-6}$		[27]
Transparency carrier amount	N_0	763500		[27]

#197315 - $15.00 USD Received 6 Sep 2013; revised 9 Oct 2013; accepted 13 Oct 2013; published 24 Oct 2013

3. Optical injection

This paper focuses on excitability in microdisk lasers that are locked using external optical injection, i.e., for sufficiently high input power the disk will lase at the same frequency of the input signal. In the unidirectional regime (at $I = 2.3$ mA), we investigated the effect of optical injection in E^+, as a function of the injection amplitude $E_{in} = E_{in,1}$ ($E_{in,2} = 0$), and the detuning $\Delta\omega$. This configuration for optical injection is identical to the one studied for SRLs in [28]. Consequently, as those SRLs are governed by the same physics, the same locking regimes appear. Indeed, the bifurcation diagram in Fig. 2 shows three stable locking regimes, in which the power does not oscillate between the two modes: U_1, U_2 and *Bi*. U_1 and U_2 stem from the positive and the negative unidirectional regime. Since power is mainly injected in the positive mode, U_1 is most prominent. The locked regime *Bi* finds its origin in one of the bidirectional solutions, which is not stable in the absence of optical injection at these currents. The size of this regime is controlled by ϕ_c, and increases for values close to $\frac{\pi}{2}$ (in this paper, $\phi_c = 0.45\pi$).

The regimes lose stability when their surrounding bifurcations are crossed, Hopf-bifurcations are denoted by red lines, saddle-node bifurcations and other limit points by blue lines. Upon crossing these bifurcations, the laser states can end up in limit cycles, or more complex (chaotic) attractors. In Fig. 2, for simplicity, we omitted the bifurcations corresponding to unstable structures or chaotic regions, as they are already extensively discussed in [28] and not important for the remainder of this paper.

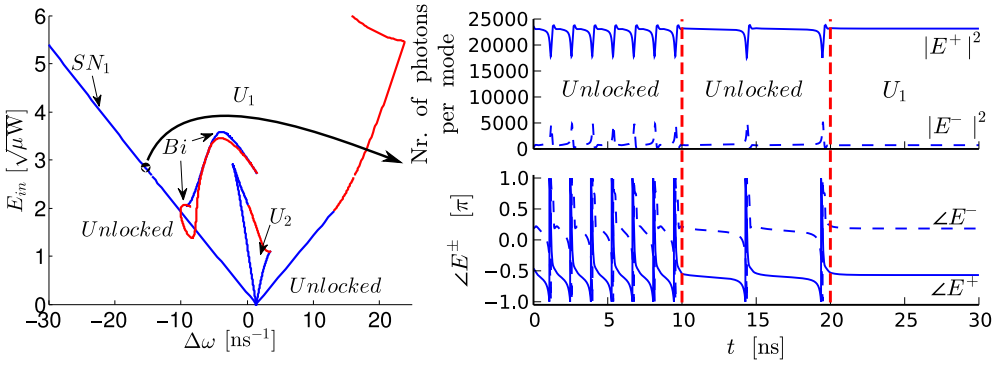

Fig. 2. Left: Bifurcation lines and locking regions for $I = 2.3$ mA, red lines represent Hopf-bifurcations, blue lines are limit points. Time traces: Crossing the SN_1 bifurcation at $\Delta\omega = -15$ ns^{-1}, $|E_{in}| = 2.77$ $\sqrt{\mu W}$. At $t = 10$ ns the locking amplitude is raised from 2.65 to 2.76 $\sqrt{\mu W}$, at $t = 20$ ns, the bifurcation is crossed by again increasing $|E_{in}|$ to 2.78 $\sqrt{\mu W}$.

In this paper, we focus on the positive unidirectional regime U_1, and the saddle-node bifurcation SN_1. This injection regime behaves identical to the one found in single-mode semiconductor lasers, which has been extensively studied [29].The time trace in Fig. 2 shows that when this bifurcation line is crossed, there is a smooth transition between an equilibrium (the locked state) and a limit cycle (the pulsing state). SN_1 is a *saddle-node bifurcation on an invariant circle* (SNIC). Such bifurcations are well-known when it comes to studying excitability in biological neurons [6].

4. Excitability

Excitability is typically defined in the context of a small perturbation at the input of a system in a stable equilibrium [28]. When the perturbation is below a certain threshold, the system re-

#197315 - $15.00 USD Received 6 Sep 2013; revised 9 Oct 2013; accepted 13 Oct 2013; published 24 Oct 2013

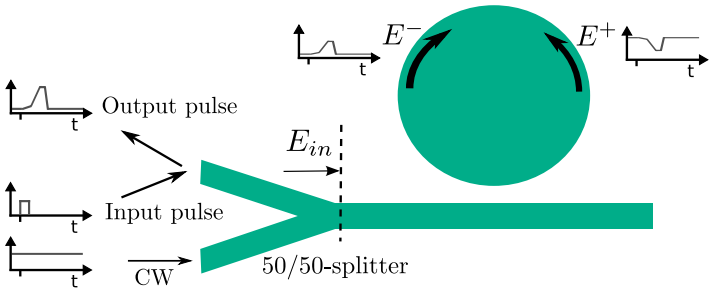

Fig. 3. The 'neuron' topology; using a constant locking signal (*CW*), the microdisk gets locked just above the SN_1-bifurcation. Pulses at the other input of the splitter, perturb the microdisk, possibly causing excitation. The energy peak in the E^- mode that comes with this excitation, can be seen as the output pulse.

sponds weakly, and fairly linear with the perturbation strength. However, when the perturbation is above threshold, and the system responds strongly, often with one or more output pulses, the system response above threshold stays nearly constant. At a SNIC-bifurcation, such as SN_1 in Fig. 2, one can find *Class I* excitability. This means that, as a response to a superthreshold step input, pulse trains are generated for which the pulse amplitude is close to invariant, whereas the pulse frequency can be made arbitrary low by choosing step heights arbitrary close to the threshold. Due to the similarity with a LIF neuron, this type of neuron behavior is very interesting from an application's viewpoint [5, 6, 8].

Figure 3 shows a topology that can be used to exploit this excitation. The *CW* input provides a constant signal that locks the microdisk just above the SN_1-bifurcation. Pulses at the other input of the splitter, cause perturbations on the locking signal. When the disk gets excited, the pulse in the suppressed mode of the laser will be visible as an upward pulse at the same port. The ability to retrieve an output signal proportional to the suppressed mode is a clear advantage with respect to the situation for a single-mode semiconductor laser as in [29], as it enhances the extinction ratio. Below, the amplitude of the locking signal $|E_{CW}| = 4.10\ \sqrt{\mu\mathrm{W}}$ is chosen so that $|E_{in}| = 2.90\ \sqrt{\mu\mathrm{W}}$, while $\Delta\omega$ for both locking signal and input pulse is $-15\ \mathrm{ns}^{-1}$.

The traces in Fig. 4(a) show the responses to square input pulses of duration 0.2 ns, with input pulse power varying from $0.6\,\mu$W to $2.2\,\mu$W. Figure 4(b) and 4(c) show the output peak power, and the output pulse latency, respectively, as function of the input pulse power. The strong threshold behavior is very clear. Above threshold, the output pulses are very prominent. The decrease of pulse peak power above threshold deviates from what is usually observed in most biological neurons, where the output pulse power typically increases slightly for further increase of the input power [6]. Also note that the pulse latency (the time between perturbation and excitation) decreases for increasingly stronger input pulses above threshold. This is a known feature for SNIC-bifurcations.

In these simulations, the input pulses had a π phase shift, relative to the *CW*-input. The influence of the phase is made clear on the traces in Fig. 4(d). Only for a limited interval around π, will the disk be excited. The sudden increase of output pulse latency, close to the edges of this region, is also noteworthy. Pulses with the same power profile can clearly cause very divergent responses, depending on their phase. Figures 4(e) and 4(f) show these trends in more detail. For completely randomized phases, only about 25% of all input pulses would result in excitation. Fortunately, the phase difference between the input pulse and the locking signal can be deliberately controlled externally. In contrast, the excitability mechanism in asymmetric SRLs without optical injection is sensitive to the phase difference between the input pulse and the laser state,

#197315 - $15.00 USD Received 6 Sep 2013; revised 9 Oct 2013; accepted 13 Oct 2013; published 24 Oct 2013

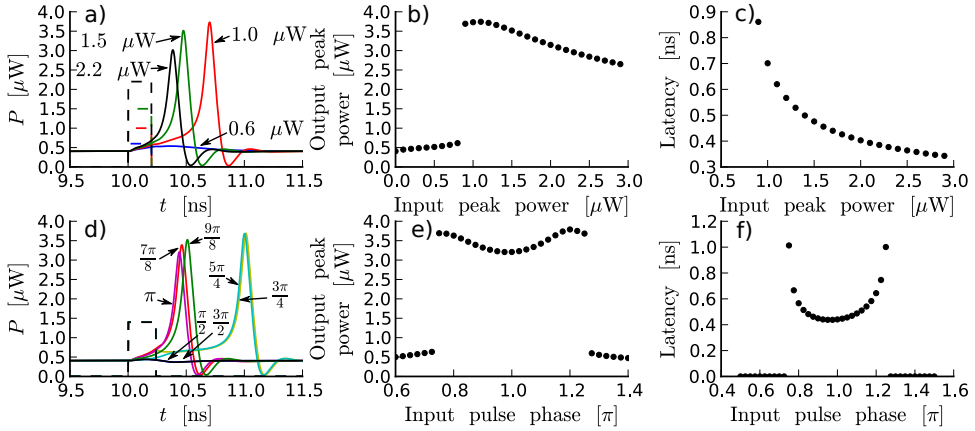

Fig. 4. a)-c) Response to pulses of fixed length (0.2 ns), for different pulse powers, out of phase with the locking signal. a: Time traces. b: Output peak power as a function of input peak power. c: Pulse latency as a function of input peak power. d)-f) Response to pulses of fixed peak power and length (1.4 μW, 0.24 ns), but varying phase. d: Time traces. e: Output peak power as a function of phase. f: Pulse latency as a function of input pulse phase.

which is uncontrollable in a practical setup [16].

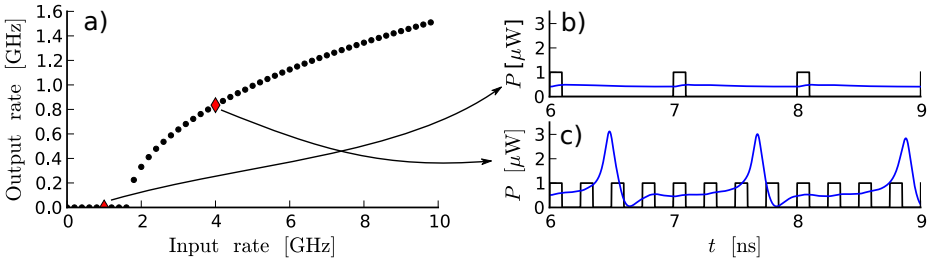

Fig. 5. a) Input rate-output rate characteristic of the neuron, when the input pulse train consists of subthreshold pulses ($|E_{in}|^2 = 1$ μW peak power, 1 ns length). b)-c) time-traces, for input rates 1 GHz (a), and 4 GHz (b). The arrows show how they are linked to points in the first graph.

One can categorize pulses as being *superthreshold*, or *subthreshold*, if they can or cannot excite the disk, respectively. Whether a pulse is superthreshold or subthreshold, will be a combined result of its amplitude, duration, phase, and the power of the locking signal. However, several subthreshold pulses can combine to form a superthreshold excitation, as long as they arrive close to each other. This is a characteristic of an *integrating neuron* [6]. Although this might seem very trivial, not all excitation mechanisms behave this way. When a subthreshold excitation causes oscillations, as is the case for Hopf bifurcations (*Class II* excitability, which appears, e.g., in passive silicon microrings [23]) the neuron will act as a resonator: multiple subthreshold excitations can only excite the system if their delay is close to an integer multiple of the natural oscillation period of the oscillations of the system. The excitation mechanism presented by Gelens, Coomans et al. [13, 15, 28] also incorporates resonator instead of integrating behavior.

#197315 - $15.00 USD Received 6 Sep 2013; revised 9 Oct 2013; accepted 13 Oct 2013; published 24 Oct 2013

Figure 5(a) shows the output-versus-input rate, for a stream of subthreshold pulses, Figs. 5(b) and 5(c) respectively show time traces of input and output pulses for two input pulse rates. The output-versus-input rate curve shows similarities with the typical sigmoidal input power versus output power characteristics of classical artificial neurons [5, 30]. This intuitively explains that spiking neural networks can have the same computational power as these classical sigmoidal networks. Due to the more intricate dynamics, it has been proven that the computational power of a spiking neural network can even be greater than that of these sigmoidal networks [5].

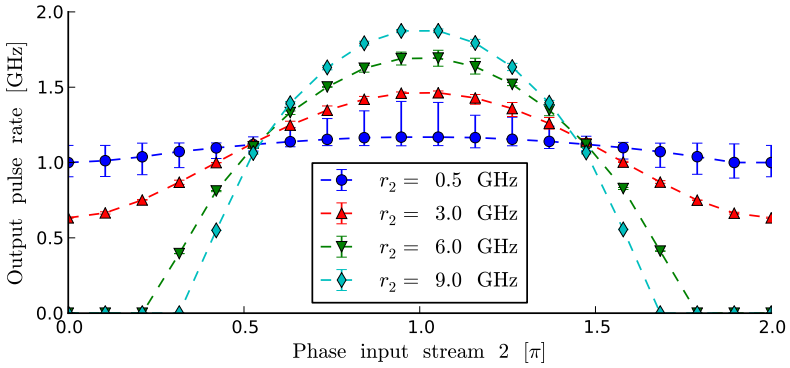

Fig. 6. Output pulse rate as response to the superposition of two input pulse streams, one stream is constant (6 GHz, 1 μW peak power and 0.1 ns duration) and purely excitatory (relative phase with respect to the *CW* is π). The other pulse stream has a varying rate r_2, the horizontal axis represents its phase. Peak power and duration are the same as for the first stream. The error bars give the 80% certainty interval for the inverse interpulse delays.

The strong phase dependency, that was apparent from Fig. 4(d)-(f) is validated by Fig. 6. Roughly speaking, pulse trains with a phase between $\frac{\pi}{2}$ and $\frac{3\pi}{2}$, have a tendency to excite the system, these pulses are called *excitatory perturbations*. Pulses with an optical phase between $-\frac{\pi}{2}$ and $\frac{\pi}{2}$ push the system's state away from the bifurcation, they are called *inhibitory perturbations*. Figure 6 shows the output pulse rate, as a response to a superposition of two input pulse streams. One of the pulse streams is kept constant, and is purely excitatory. The rate and the phase with respect to the locking signal of the other stream are varied. Every line on the graph represents a specific rate of the second pulse stream r_2, for which the phase is shown on the horizontal axis. The constant pulse train by itself, would give rise to an output pulse rate of about 1.12 GHz (see Fig. 5(a)). A second input pulse train can clearly affect this output pulse rate. Inhibitory pulses tend to reduce the rate, excitatory pulses increase it. The higher the pulse rate, and the closer the phase of the second pulse train to π (purely excitatory) or 0 (purely inhibitory), the bigger the effect. This behavior makes rudimental operations such as (nonlinear) 'addition', or 'subtraction' of pulse rates, possible. Phase control of the optical links in a disk network could be controlled using, e.g., heaters [31].

Finally, whereas the excitation mechanism proposed in [13, 28] is heavily dependent on the precise phase ϕ_c of the intermodal coupling, while ϕ_c is not straightforward to control during fabrication, the currently proposed excitation mechanism is less sensitive to this value, as ϕ_c has less influence on the threshold for optical injection than on the onset of AO.

#197315 - $15.00 USD Received 6 Sep 2013; revised 9 Oct 2013; accepted 13 Oct 2013; published 24 Oct 2013

5. Future prospects

In future work, the transfer of excitation between different disks will be investigated. Amongst other fabrication imperfections, the ability of the neuron to react on the phase of the input pulses, makes larger microdisk networks sensitive to phase errors. Consequently, even though an integrated platform intrinsically limits the variable phase noise, one still needs a reliable, power efficient way to compensate for fixed phase offsets in large microdisk network.

6. Conclusions

Optically injected microdisk lasers can exhibit class I excitability. With the right geometry, this excitability mechanism can be addressed. The excitability mechanism shows similar properties to equivalent class I excitability found in biological neurons. Other properties, such as strong influence of optical phase, however, have no equivalent in biological or electrical systems, though they greatly influence the behavior of this specific excitability mechanisms. In the presented geometry, both output and input are signals with relatively strong power pulses on a small background signal. The similarity between input and output is expected to make excitation transfer between different disks possible.

Acknowledgments

This work is supported by the interuniversity attraction pole (IAP) Photonics@be of the Belgian Science Policy Office and the ERC NaResCo Starting grant. T. Van Vaerenbergh is supported by the Flemish Research Foundation (FWO-Vlaanderen) for a PhD Grant.

#197315 - $15.00 USD Received 6 Sep 2013; revised 9 Oct 2013; accepted 13 Oct 2013; published 24 Oct 2013